Electronic Supplementary Information

Correlative Dual-Alternating-Color Photoswitching Fluorescence Imaging and AFM Enable Ultrastructural Analyses of Complex Structures with Nanoscale Resolution

Jie Wang,[†] Zicheng Wang,[†] Yangyue Xu,[‡] Xuefei Wang,[†*] Zhiyong Yang,[†] Hongda Wang,[‡*] Zhiyuan Tian[†*]

[†]School of Chemical Sciences, University of Chinese Academy of Sciences (UCAS) Beijing 100049, PR China, E-mail: xfwang@ucas.ac.cn, zytian@ucas.ac.cn

[‡]State Key Laboratory of Electroanalytical Chemistry, Changchun Institute of Applied Chemistry, Chinese Academy of Sciences (CAS), Changchun 130022, PR China, E-mail: hdwang@ciac.jl.cn

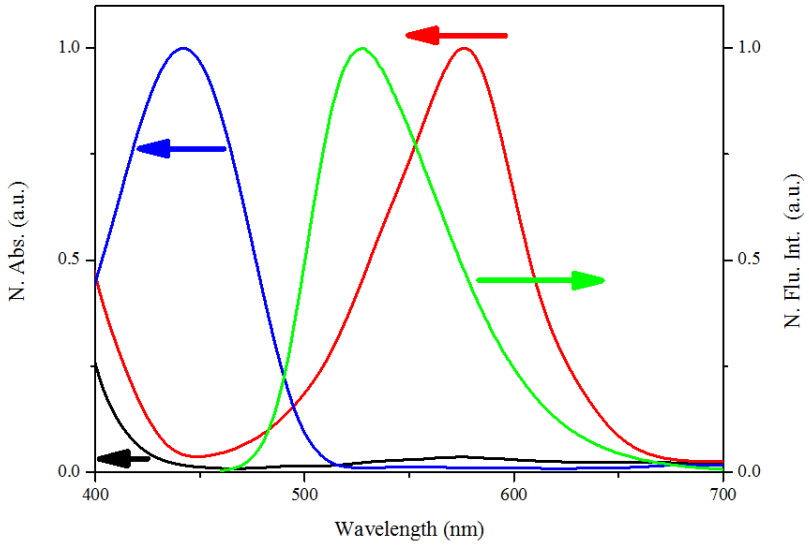

Figure S1. UV-visible absorption spectra of naphthalimide (blue curve), SP (black curve) and MC (red curve) in acetonitrile and fluorescence emission spectrum of naphthalimide (green curve, ex: 440nm).

The green fluorescence on/off photoswitching of naphthalimide is dependent on the FRET process controlled by irradiation of alternative UV or visible light. Generally, naphthalimide unit (energy donor) cannot transfer its excitation energy to SP (energy acceptor) because the emission of naphthalimide has poor overlap with the absorption spectra of SP (green curve and black curve).When SP is converted to MC by exposure to UV light, the FRET process between the naphthalimide to the MC is activated due to a new absorption band of MC centered at 575 nm, which overlaps appreciably with green emission band of the naphthalimide unit (green curve and red curve). Besides, MC (red curve) have a weak absorption intensity at 440 nm and it means that the excitation wavelength of green channel at 440 nm cannot effectively activate MC.

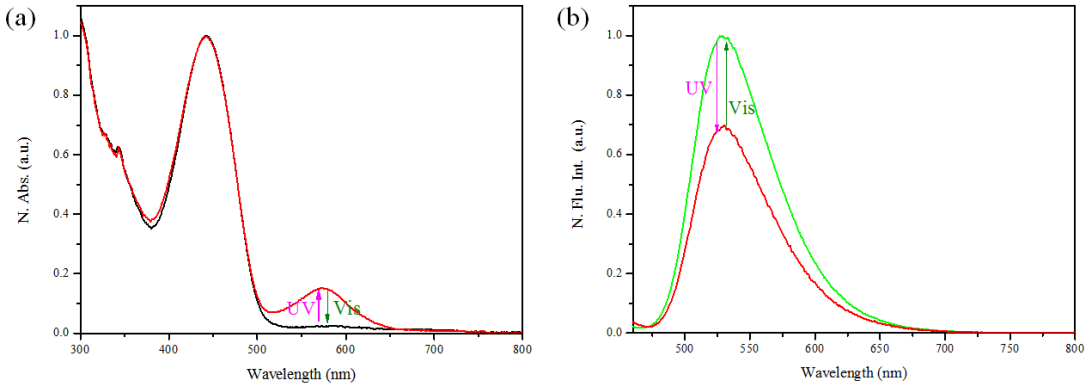

Figure S2 (a) UV-vis absorption and (b) fluorescence photoswitching of NI-SP in acetonitrile (ex: 440 nm). Note that NI-MC in common organic solvents or aqueous systems fluoresces weakly in the red channel.

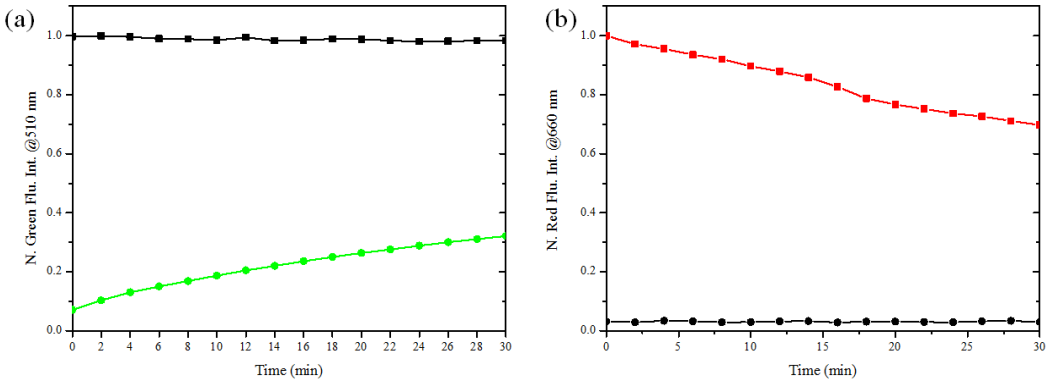

Figure S3. Thermally driven (a) green fluorescence and (b) red fluorescence of NI-SP in PMMA film (monitored at 510 nm and 650 nm respectively, ex: 440 nm and 560 nm). The bright state in green channel is stable, however, in the dark state 30% of the fluorescence recovers 30 min later (Figure S3-a). Opposite to the green channel, the red fluorescence shows the intensity decays 28% after UV illuminates and the dark state has no significant changes in 30 min (Figure S3-b).

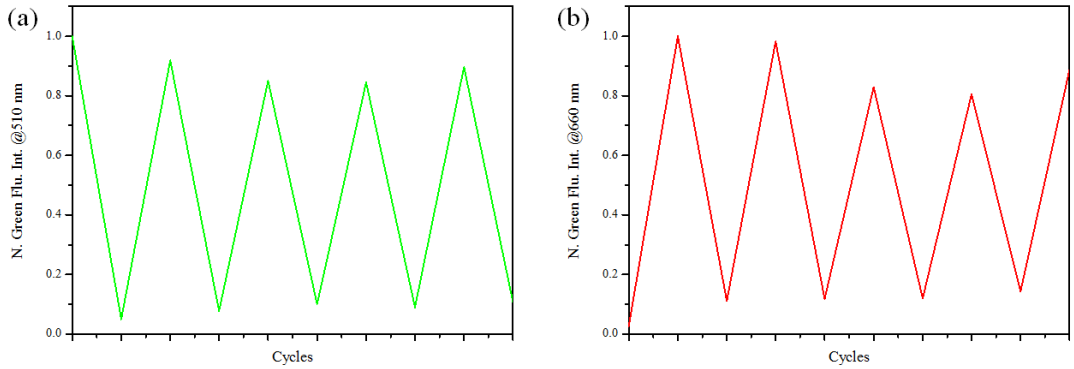

Figure S4. Modulation of the intensity of (a) green fluorescence at 510 nm and (b) red fluorescence at 650 nm with alternating UV and visible light.

The repeatability of green and red fluorescence photoswitching of NI-SP doped PMMA film was evaluated by monitoring the green fluorescence intensity (at 510 nm) and the red fluorescence intensity (at 660 nm) under illumination of alternating UV and visible light. Specifically, the intensities of the sample in NI-SP configuration were acquired following 30 s illumination of UV (365 nm) light from a handheld lamp; and those in NI-MC configuration were acquired 1 minutes illumination of LED light at 50 ℃ using a filter for blocking the light with wavelength less than 525 nm. It can be seen from Figure S4 that for several cycles, the modulation of dual-color fluorescence was nearly fully reversible, demonstrating the well-behaved on-and-off fluorescence switching properties and photostability of NI-SP doped film.

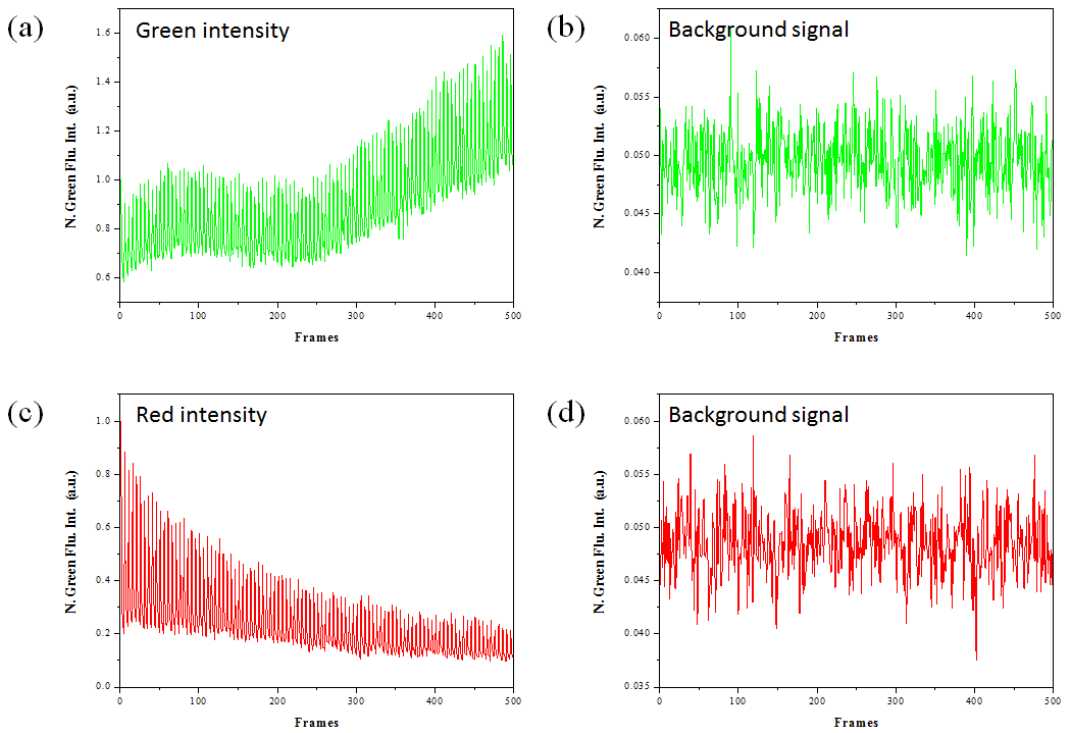

Figure S5. Photoswitching cycles of PSMA NPs doped by NI-SP. (a) The cycles of green fluorescence changes upon 405 nm laser excitation and 561 nm laser activation every 5 frames. (b) The cycles of red fluorescence upon 561 nm laser excitation and 405 nm laser activation every 5 frames. Both of green and red fluorescence intensity reveals on/off modulation pattern for well-behaved photoswitching behavior. But a plot of the background spot in green (b) and red (d) channels reveals no regular periodicity.

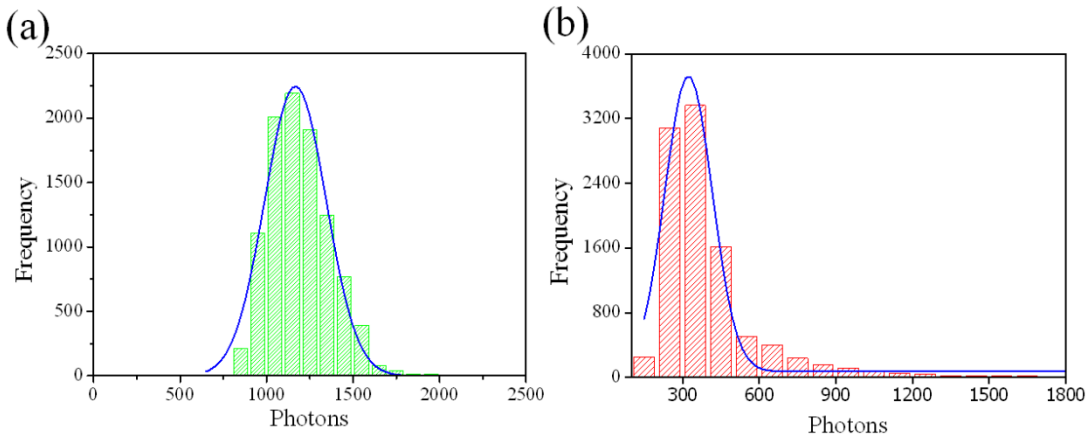

Figure S6. Histograms of the detected numbers of photons per switching event in green- (a) and red-channel (b) of a single NI-SP molecule in PMMA film.

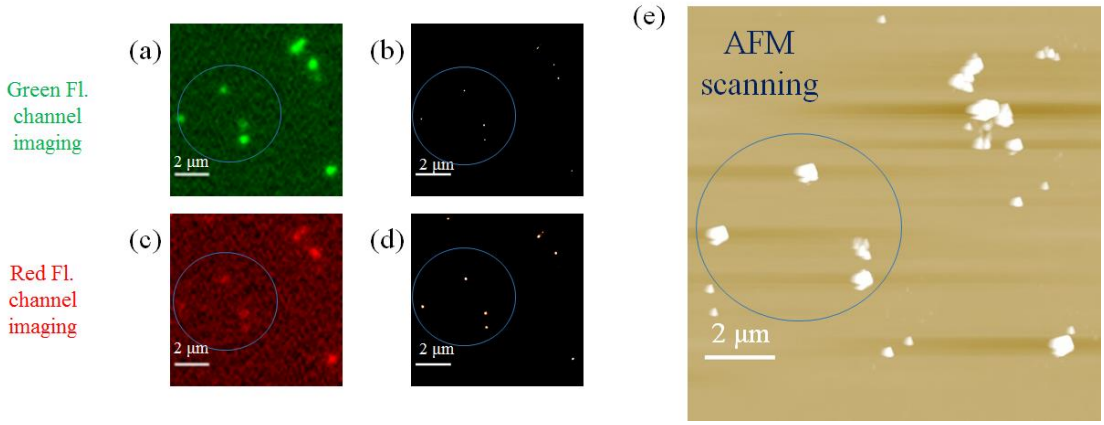

Figure S7. Correlative super-resolution imaging and AFM scanning of PSMA NPs labeled by NI-SP. (a), (c) Conventional fluorescent images of the NPs in green and red channels respectively. (b), (d) Super-resolution fluorescence imaging of these NPs in green and red channels. (e) AFM scanning of the same region. From the figures, most of the NPs in fluorescent images identically seen in the AFM images. The super-resolution fluorescent images provide clear visualization of the targeted NPs labeled by NI-SP, and meanwhile the AFM images provide morphology information of the NPs.

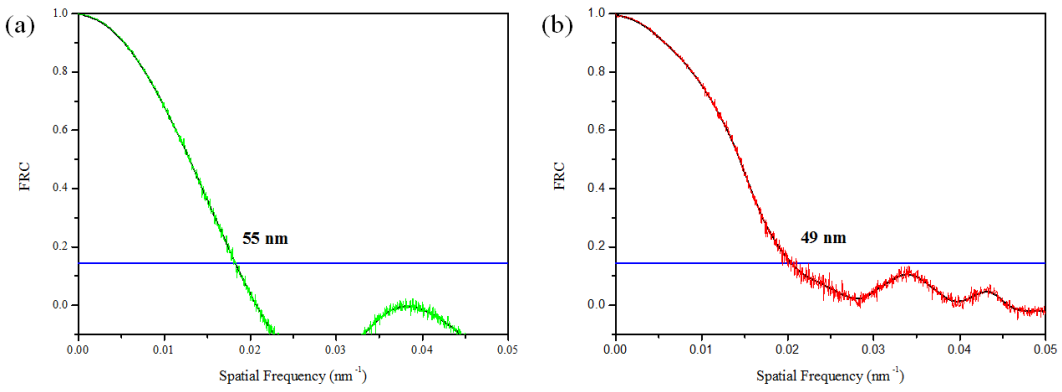

Figure S8. Fourier ring correlation (FRC) analysis of PSMA NPs doped by NI-SP in (a) green channel and (b) red channels presented in Figure 4b and f. The resolution of the images is calculated 55 nm in green channel and 49 nm in red channel from the intersection between the FRC smoothed curve (black curve) and the fixed (1/7) threshold (blue curve), green and red curves are FRC noisy data in both channels.

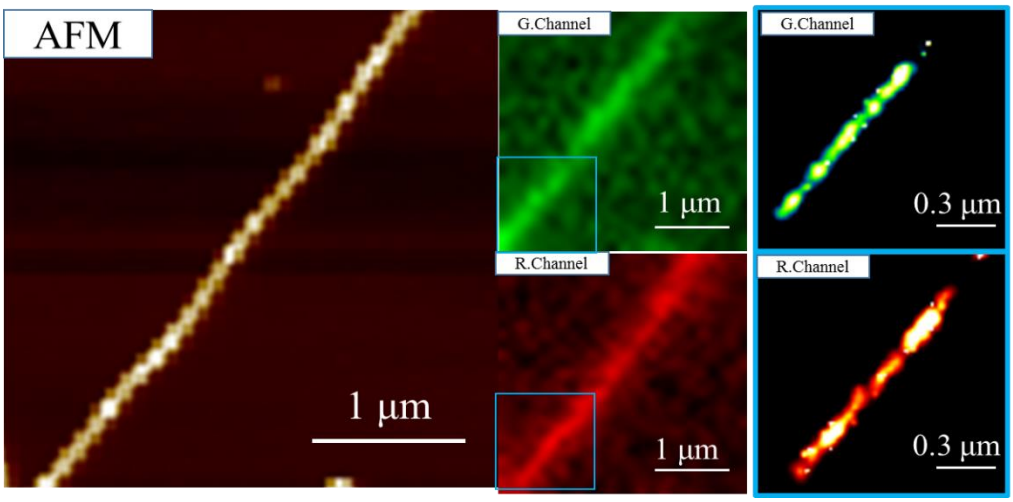

Figure S9. Correlative super-resolution imaging and AFM scanning of PSt-b-PEO copolymer micelles labeled by NI-SP.

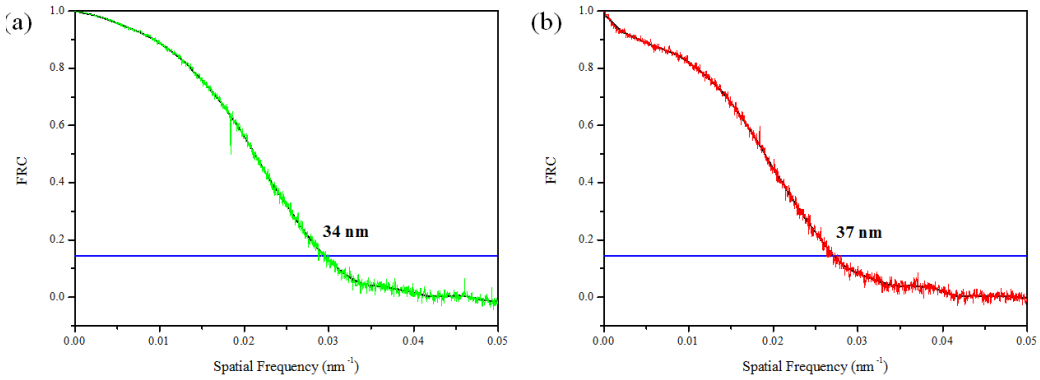

Figure S10. Fourier ring correlation (FRC) analysis of PSt-b-PEO copolymer micelles doped by NI-SP in (a) green channel and (b) red channels presented in Figure 5b and f. The resolution of the images is calculated 34 nm in green channel and 37 nm in red channel from the intersection between the FRC smoothed curve (black curve) and the fixed (1/7) threshold (blue curve), green and red curves are FRC noisy data in both channels.

Experimental section

Materials. Poly(styrene-co-maleic anhydride) (PSMA) was purchased from Sigma-Aldrich and polystryrene-block-poly(ethylene oxide) (PSt-b-PEO) was obtained from Polymer Source. Anhydrous tetrahydrofuran (THF) and dichloromethane (CH_2Cl_2) were purchased from Energy Chemistry. Other reagents and solvents were commercially available and used directly without further purification.

Synthesis and Characterizations

Synthesis of SP-COOH (1). As illustrated in Figure S11, the SP-COOH, namely 3-(3', 3'-dimethyl-6-nitrospiro [chromene-2, 2'-indolin]-1'-yl) propanoic acid (1), was synthesized according to the literature.[1,2]

Synthesis of Compound 2.[3,4] A mixture of 4-bromo-1, 8-naphthalic anhydride (10 mmol, 2.8 g) and 3-aminophenol (15 mmol, 1.6 g) was added to ethanol (20 mL) and the resulting solution was refluxed overnight. After cooled down to room temperature, the faint yellow product was filtered off and further purified by column chromatography (eluent: ethyl acetate/hexane (1:3)), yielded compound 2 as a grey powder (2.6 g, yield: 72%). ^{1}H NMR (400 MHz, DMSO‑d_6) δ9.62 (s, 1H), 8.59-8.51 (m, 2H), 8.31 (d, J =8.0 Hz, 1H), 8.22 (d, J =7.9 Hz, 1H), 7.99 (t, J = 7.9 Hz, 1H), 7.26 (t, J=8.3 Hz, 1H), 6.84 (d, J= 9.3Hz, 1H), 6.79-6.70 (m, 2H).

Synthesis of Compound 3.[5] Azetidine (10 mmol, 580 mg) was added dropwise to 10 mL 2-methoxyethanol solution of compound 2 (2 mmol, 0.74 g) and the solution was refluxed for 2 h. After the solution was cooled to room temperature, the product was filtered off and then washed with hexane to give orange-yellow crystals 3 (400 mg, yield 58%).[5] ^{1}H-NMR (DMSO‑d6, 400 MHz) δ8.42-8.34 (m, 2H), 8.18 (d, J=8.5 Hz 1H), 7.59 (t, J = 7.9 Hz, 1H), 7.23 (t, J = 8.0 Hz, 1H), 6.80 (d, J = 8.2 Hz, 1H), 6.80-6.71 (m, 2H), 6.47 (d, J = 8.6 Hz, 1H) 4.48 (t, J = 7.5 Hz, 4H), 2.55-2.41 (m, 2H).

Synthesis of NI-SP.[6] 0.38 g compound 1 (1 mmol), 0.35 g compound 3 (1mmol) and 3mg DMAP were dissolved in anhydrous CH_2Cl_2 (50 mL); the resulting solution was added into a 100mL flask and the mixed solution was cooled down to 0 ℃. After 3-min stirring, EDC was added to the reaction mixture and stirred for another 5 min at 0 ℃. Then the solution was warmed up to room temperature and stirred overnight. After filtration the solution was washed using 1 M HCl solution and then saturated $NaHCO_3$ solution, respectively, and subsequently dried using $MgSO_4$. The product was then purified by flash column chromatography (eluent: petroleum ether/ethyl acetate (4:1) to CH_2Cl_2/ethyl acetate (20:1)), yielding the target compound NI-SP (84

mg, yield 12%). ^{1}H-NMR (DMSO‑d6, 400 MHz) δ8.46-8.35 (m, 2H), 8.21-8.14 (m, 2H), 7.95 (d, J=8.9 Hz, 1H), 7.61 (t, J = 7.7 Hz, 1H), 7.45 (t, J = 8.0 Hz, 1H), 7.22-7.15 (m, 2H),7.12-1.05 (m, 3H), 7.02 (s, 1H), 6.86 (d, J = 9.0 Hz, 1H), 6.78-6.68 (m, 2H), 6.50 (d, J = 8.4 Hz, 1H), 6.01 (d, J=10.4 Hz, 1H), 4.48 (t, J = 7.4 Hz, 4H), 3.64-3.45 (m, 2H), 2.99-2.72 (m, 2H), 2.51-2.42 (m, 2H), 1.15 (s, 3H), 1.05 (s, 3H).

Preparation of NI-SP-doped PSMA Nanoparticles (NPs).[7] NI-SP-doped PSMA NPs were prepared via a reprecipitation strategy. In a typical protocol, 50 μL PSMA/THF solution (1 mg/mL) and 2.5 μL NI-SP/THF (0.1 mg/mL) were added to 10 mL THF, and the obtained homogeneous solution was rapidly added to 20 mL of Milli-Q water in an ice bath. Upon subsequent 5-min sonication and then nitrogen bubbling for removing THF at room temperature, aqueous sample with NI-SP-doped PSMA NPs dispersed in water was obtained.

Preparation of PSt-b-PEO Block Copolymer Micelles.[8] A homogeneous solution containing PSt-b-PEO and NI-SP was prepared by dissolving 10 mg of PSt-b-PEO and 0.2 mg of NI-SP in 1mL chloroform with sonication. 0.1 mL of the abovementioned solution was slowly added to an open flask with 1 mL of 1mg/mL sodium dodecyl sulfate (SDS) aqueous solution and the mixture was kept in an ice bath and stirred overnight to remove chloroform. After filtering off the residues, the aqueous dispersion sample was centrifuged at 7000 rpm for 30 minutes twice and the obtained precipitate was dissolved in 1mL water and then dropped on a clean coverslip for the correlative imaging.

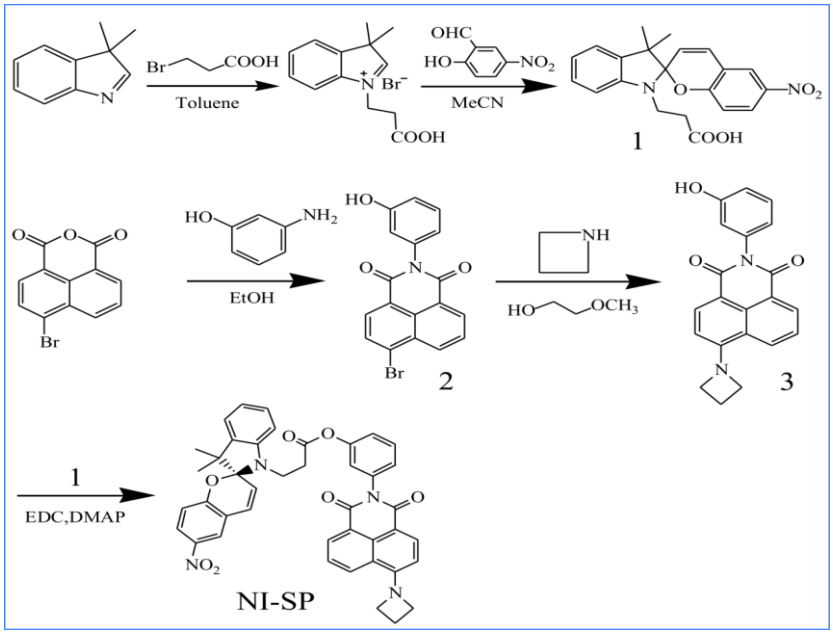

Figure S11. Synthesis route of photoswitchable NI-SP dyad.

Correlative dcPSF-AFM Imaging of PSMA NPs and PSt-b-PEO Micelles.

The correlative microscope was based on a commercially available platform that integrates AFM (Keysight 7500) on a homebuilt inverted optical microscope unit, which has been adapted for super-resolution imaging as previously described (Figure S12). Samples were excited and photoswitched with 405 and 561nm lasers (Coherent OBIS^{TM}) and imaged onto an electron multiplying charge coupled device (EMCCD) camera (iXon Ultra 888, Andor Technology) through a 100×, 1.30 numerical aperture oil immersion objective (Nikon). Super-resolution imaging and AFM scanning are performed sequentially.

For dcPSF imaging of samples, the samples were placed onto the AFM platform that mounted onto the microscope objective. The two lasers were reflected into the objective by a 45° dual-edge laser-flat dichroic beam splitter (Chroma, ZET405/488/561/640m). The scattering and reflection from the 405 nm laser were further cleaned up by the long-pass filter that cut off at 412 nm (Chroma, T412lpxt). The green and red fluorescence were purified using a short pass filter that cuts off at 600 nm (Chroma, ET600sp) or a long pass filter that cuts off at 573 nm (Semrock, FF573-Di01-25×36). The dcPSF image was collected by a highly sensitive electron multiplying charge coupled device (EMCCD) camera. In green channel, the 405 nm

imaging laser and CCD camera were turned on simultaneously for 50 ms to capture the bright green fluorescence image. To switch off the fluorescence, the 405 nm laser was turned on for an additional 50 ms. Then 100 ms dark treatment turned on the green fluorescence again, thus completing one photoswitching cycle. In red channel, The 405 nm laser was switched on for 2 ms to turn on red fluorescence. Then the 561 nm imaging laser and CCD camera were turned on simultaneously for 50 ms to capture the bright red fluorescence image. To switch off the fluorescence, the 561 nm laser was turned on for an additional 50 ms. Usually, 200 frame images were taken by the CCD with a speed of 0.05 s per frame in both green and red channels. Thus it took about 70 s for dcPSF imaging. The obtained movies were analyzed to reconstruct super-resolution images with the ThunderSTORM plugin for ImageJ.

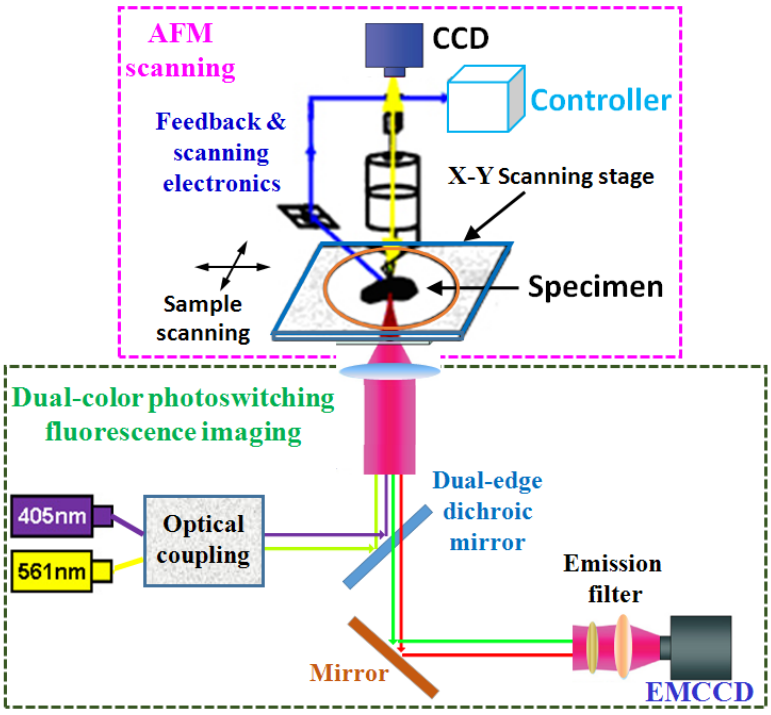

Figure S12. Diagram of the experimental setup for correlative AFM and super-resolution fluorescence microscopy. The instrument setup consists of AFM units and fluorescence imaging units, and the critical correlation of these devices is the aligned optical path with the AFM cantilever to guarantee the same region of the two imaging modes.

AFM experiments were conducted in tapping mode using Silicon-SPM-Sensor cantilevers (Nanosensors, Switzerland) with a typical force constant of 40 N/m and a

resonance frequency of 167 KHz under dry conditions. Images were taken at a resolution of 1024 × 1024 and a rate of 0.7 s/line.

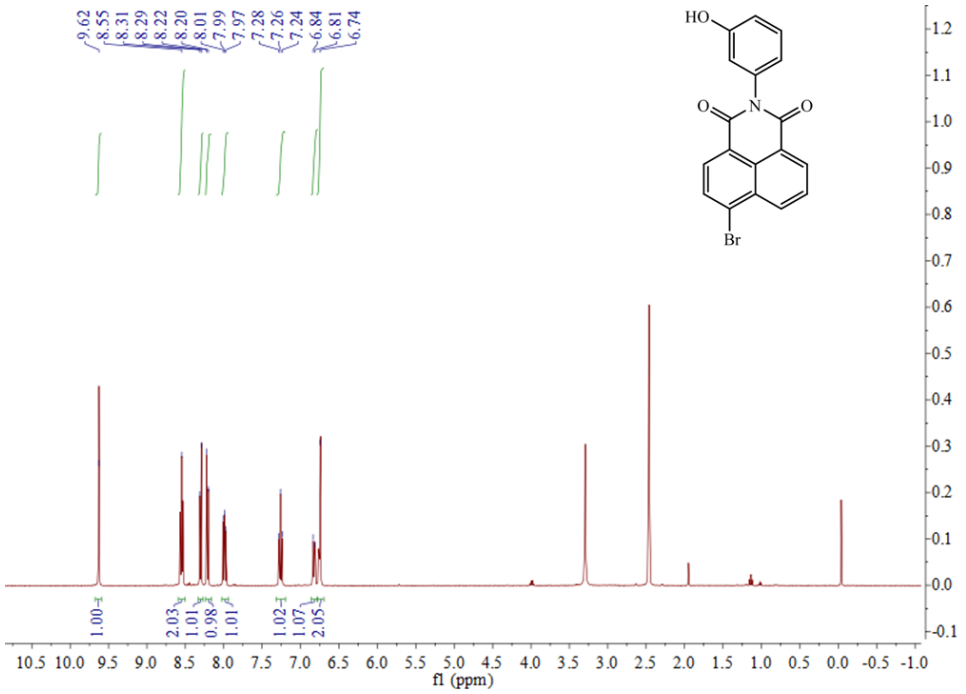

Figure S13. ^{1}H NMR spectrum of 6-bromo-2-(3-hydroxyphenyl)-1H-benzo[de]isoquinoline-1,3(2H)-dione (compound 2) in DMSO-d6.

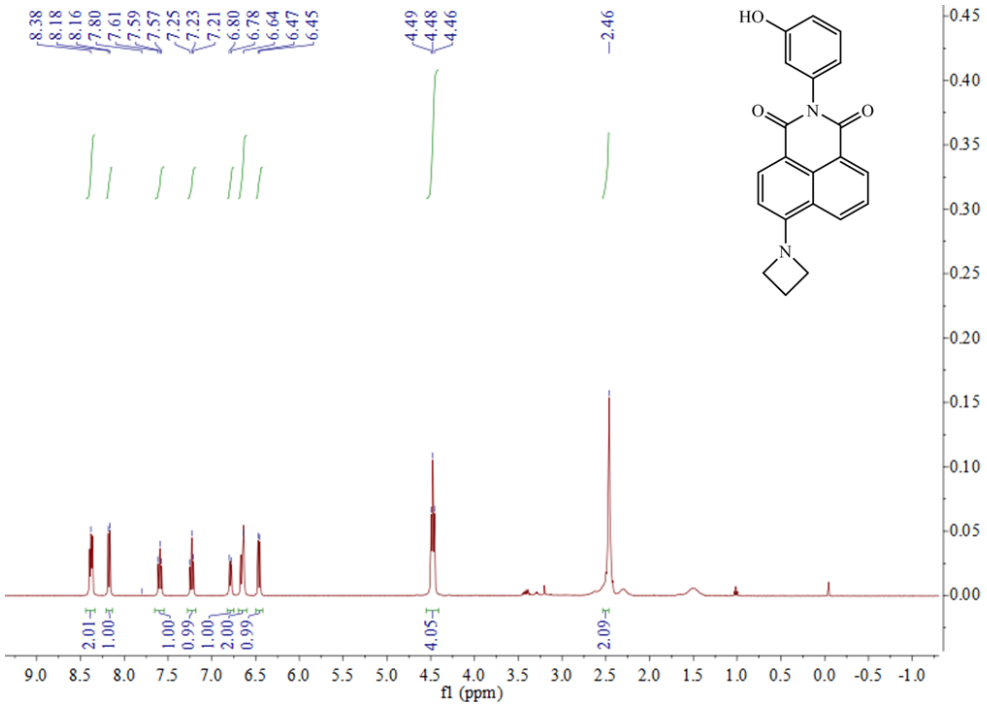

Figure S14. ^{1}H NMR spectrum of 6-(azetidin-1-yl)-2-(3-hydroxyphenyl)-1H-benzo [de]isoquinoline-1,3(2H)-dione (compound 3) in DMSO-d6

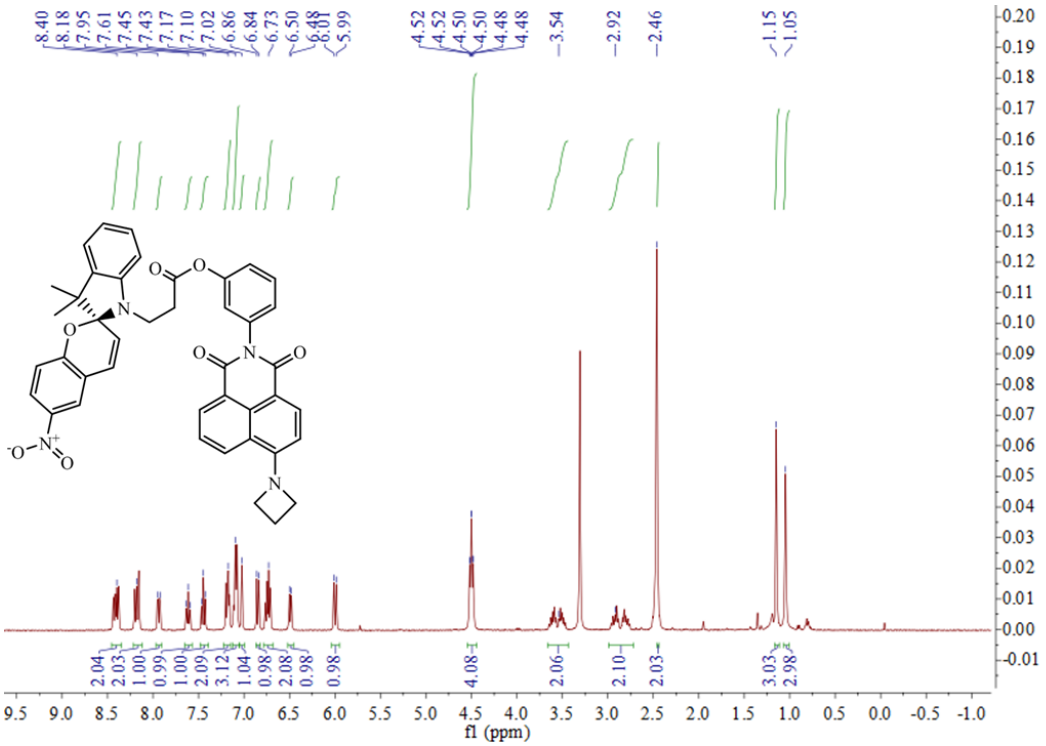

Figure S15. ^{1}H NMR spectrum of 3-(6-(azetidin-1-yl)-1,3-dioxo-1H-benzo[de]isoquinolin-2(3H)-yl)phenyl 3-(3',3'-dimethyl-6-nitrospiro[chromene-2,2'-indolin]-1'-yl) propanoate (NI-SP) in DMSO-d6

References

1 Qingkai Qi, Chong Li, Xiaogang Liu, Shan Jiang, Zhaochao Xu, Richmond Lee, Mingqiang Zhu, Bin Xu, and Wenjing Tian, *J. Am. Chem. Soc.*, 2017, 139, 16036.

2 Zhaowei Chen, Li Zhou, Wei Bing, Zhijun Zhang, Zhenhua Li, Jinsong Ren, and Xiaogang Qu, *J. Am. Chem. Soc.*, 2014, 136, 7498.

3 Kyung-Won Kim, Geun-Hyeong Kim, Su-Hyeon Kwon, Hyo-In Yoon, Jung-Eek Son, Jae-Hong Choi, *Dyes and Pigments*, 2018, 158, 353.

4 Bin Ren, Yongying Yang, Yi Qu, Jian Cao, Yuandong Wu, *Journal of Molecular Structure*, 2019, 1193, 131.

5 Xiaogang Liu, Qinglong Qiao, Wenming Tian, Wenjuan Liu, Jie Chen, Matthew J. Lang, and Zhaochao Xu, *J. Am. Chem. Soc.*, 2016, 138, 6960.

6 Zeynep Ekmekci, Betul Ulu, Evren Ekmekci, *Sensors and Actuators B*, 2016, 231, 655.

7 Liheng Feng, Libing Liu , Fengting Lv, Guillermo C. Bazan, and Shu Wang, Adv. Mater. 2014, 26, 3926.

8 Jintao Zhu and Ryan C. Hayward, *J. Am. Chem. Soc.*, 2008, 130, 7496.